

We are IntechOpen, the world's leading publisher of Open Access books Built by scientists, for scientists

6,900

Open access books available

186,000

International authors and editors

200M

Downloads

Our authors are among the

154

Countries delivered to

TOP 1%

most cited scientists

12.2%

Contributors from top 500 universities



WEB OF SCIENCE™

Selection of our books indexed in the Book Citation Index
in Web of Science™ Core Collection (BKCI)

Interested in publishing with us?
Contact book.department@intechopen.com

Numbers displayed above are based on latest data collected.
For more information visit www.intechopen.com



Human-Induced Geo-Hazards in the Kingdom of Saudi Arabia: Distribution, Investigation, Causes and Impacts

Ahmed M. Youssef, Hasan M. Al-Harbi,
Yasser A. Zabramwi and Bosy A. El-Haddad

Additional information is available at the end of the chapter

<http://dx.doi.org/10.5772/66306>

Abstract

Different types of geological hazards are induced by human activities in the Kingdom of Saudi Arabia (KSA). These geological hazards include land subsidence and earth fissures, sinkholes, expansive soils, and flash floods. A wide variety of recent geological hazards have been reported in several areas, causing significant human and property losses. Human activities, most notably groundwater extraction, infrastructure development, and agricultural activities, have induced unstable conditions. This chapter provides an overview of the human-induced geological hazard in the KSA, mainly earth fissures and sinkhole, which represent a scarcely explored topic. This work identifies the main types of human-induced geological-hazard formations, distribution, causes, and impacts, illustrated through several case studies in the KSA.

Keywords: earth fissures, sinkholes, human induced, KSA

1. Introduction

Most frequent types of geological hazards observed in the Kingdom of Saudi Arabia (KSA) can be categorized into sand accumulations; land subsidence and earth fissures; flash floods; problematic soils; slope-stability problems; karst problems; faults; volcanic activities; and earthquake hazards. These hazards can be either natural or human-induced. Most of these hazards have been recorded in the KSA [1]. In this chapter, two types of geological hazards that are induced by human activities will be discussed. These hazards include earth fissures and sinkholes. Different types of problems associated with earth fissures and sinkholes, including water leakage in reservoirs, instability problems, flooding, infrastructure and urban-

area damage, and loss of human life were recognized and evaluated by many authors [2–9]. The government of the KSA has also contributed to the extensive program of the agricultural activities for the past few decades [10]. These agriculture activities are considered as being of the largest water consumption, leading to the fast rate of depletion of nonrenewable groundwater. Analyzing the situation, it was found that: (1) during the period from 1976 to 1993, the area of agricultural land increased from 1600 to 32,000 km² and was irrigated with fossil groundwater; (2) water extracted from the aquifer was doubled between 1985 and 1990, reaching around 21,000 million cubic meters (MCM)/year. Consequently, a significant drop in the groundwater level was recorded in many regions (e.g., 100 m in the northwest area of the KSA); (3) it is expected that at the present rates of groundwater extraction, most of the fossil water will be depleted within 25–30 years. Earth fissures and sinkholes (related to carbonate and evaporite rocks) are considered to be the most-frequently observed and occurring geohazards in the KSA. The associated damage due to earth fissures and sinkholes are expected to increase in the future due to the anthropogenic alterations and the expansion of development. It was found that from years 2000–2010, the population has increased dramatically and a significant proportion of the population occupy karst areas of the eastern part of the country (e.g., Ar Riyadh) that leads to increase of vulnerability with respect to human-induced hazards. Different studies were performed in the KSA dealing with earth fissures and sinkholes [1, 11–18]. Many authors indicated that the main karst units in the Arabian Platform are Arab, Hith, Sulaiy, Aruma (Badanah, Zallum), Umm er Radhuma, Rus, Dammam, Dam, and Sirhan Formations [10, 12–14, 19].

2. Case-study group 1: earth fissures

2.1. Earth fissures' backgrounds

Earth fissures and the associated subsidence represent a major problem in different countries. Earth fissures and ground subsidence are related to the downward ground-surface movement compared with surrounding areas, ranging from strain cracks to large faults, starting from the ground surface in uncemented sediments [20, 21]. Earth fissures start from great depths below the surface, as a result of horizontal movement in the aquifers, because of excessive withdrawal (pumping) of the groundwater from the uncemented reservoir layers, due to loess soil, and earthquake activities [22, 23]. These earth fissures and subsidence could cause many problems in different urban and agricultural areas as well as damage infrastructure [24, 25]. Holzer [26] indicated that earth fissures can extend for a distance of tens of meters to kilometers due to tensile stresses. Under arid desert conditions, the shortage of groundwater resources and excessive pumping may cause continuous decline in groundwater levels [27]. When the aquifer is formed of unconsolidated sediments of high porosity and is interbedded with clay aquitards of low permeability and high compressibility, the rapid lowering of the groundwater level may also cause subsidence and possible ground failure in the form of earth fissures. Many authors documented that earth fissures and land subsidence can be related to groundwater withdrawal [28–35].

2.2. Human-induced earth fissures in the KSA

Earth fissures can be formed in loess soil due to water effect (rain, storms, floods, or leakage from agricultural irrigation channels and/or from neighboring houses). Earth-fissure and land-subsidence problems were reported in several areas in the Kingdom of Saudi Arabia causing damage to infrastructures, buildings, and agricultural areas (**Figure 1**). There are many examples of loess-related failures (earth fissures and subsidence) in the KSA such as the areas north of Jizan city, El-Darb Area, and North of Al-Nai village of Hail Region [1]. Many areas in the KSA are suffering from excessive groundwater extraction and are consequently subjected to land subsidence and earth fissures [1, 36–43]. Different types of earth fissures were detected in the KSA according to various reasons, among them are (a) earth fissures associated with groundwater extraction for agricultural development such as in Wadi Najran, Wadi El Dawather, Hail Region, Qasim Region, and Al Jouf Region; (b) earth fissures that are related to clay deposits (swelling and compressed clay deposits) such as in Hail, Al Qasim, and Al Jouf Regions; (c) earth fissures due to the Khabra deposits, which appear due to the drying effect such as in Al Jouf, Hail, and Al Qasim Regions; (d) earth fissures that are related to geological structures and groundwater withdrawal; and (e) earth fissures that are due to earthquake effects (El Shaqa area, northwest of El Madinah).

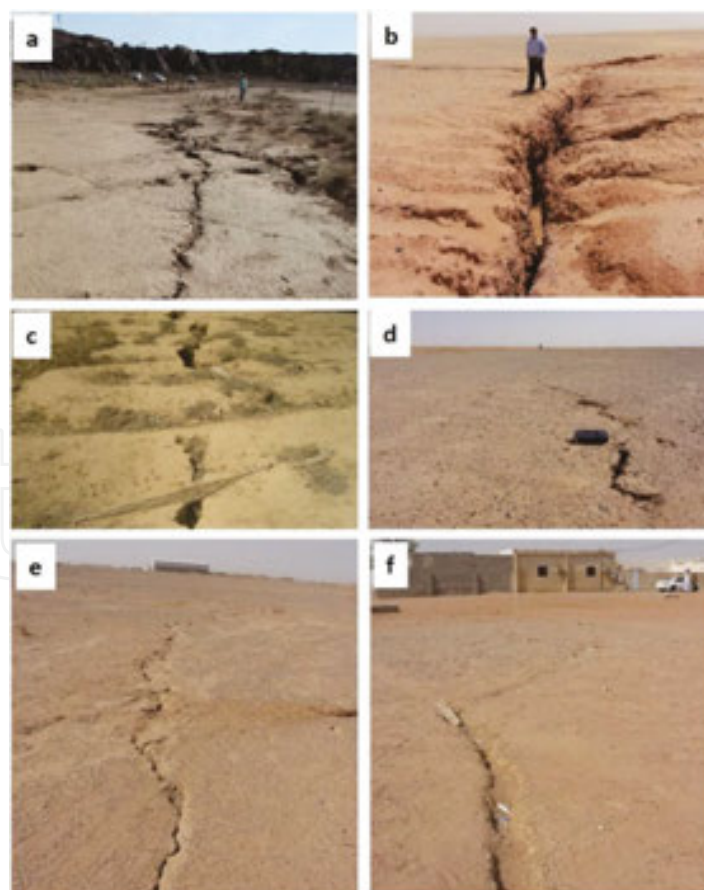


Figure 1. Earth fissures distributed in different areas in the KSA.

2.3. Earth fissures in Tabah village

2.3.1. Tabah area

The old village of Tabah is located ~70 km southeast of the Hail city at a latitude of 27° 02'N and a longitude of 42° 10'E (**Figure 2a**). It is laid on Harrat Hutaymah in an ancient volcanic crater (**Figure 2b**). This crater has dimensions of ~1.7 km by ~1.5 km and is filled with fine sediments and gravel (eroded from the surrounding volcanic tuffs), subsequently, filled with water forming a groundwater aquifer. The aquifer has been used since few decades until now by the village for drinking and irrigation. The crater has a low rim where weakly lithified tuff is exposed. Some Precambrian rocks and dikes are exposed inside the crater due to the erosion of tuff materials to fill the volcanic vent. The earth fissures are located in the old village of Tabah, which lies about 1 km southwest of the new Tabah village (**Figure 2b**). These earth fissures have been recognized and recorded since 1984. Extensive field investigations have shown the presence of earth fissures in different types, lengths, shapes, and directions (**Figure 3a**). Most of them are shown as ring shapes, forming a concentric zone along the margins of the volcanic vent (with a dimension of ~0.9 by ~0.7 km). They are deep, wide-open, and long fissures (more than 4 m deep, 3 m wide, and 600 m long). They spread in the floor of the village, agricultural areas, and cut through buildings (**Figure 3b**). Most nearby buildings and agricultural areas were damaged by these earth fissures. The presence of the earth fissures in the area leads to migration of most of the population to other areas (New Tabah village). There are some previous studies conducted in this area such as detailed in Refs. [24] and [36]. These studies indicated that the first earth fissures that were 120 m long were observed in 1981. Roobol et al. [24] mentioned that extensive earth fissures (as long as 500 m long) happened in 1984, causing damage to buildings. The present typical situation of these earth fissures is shown in (**Figure 2b**). The earth fissures in the area are shown as concentric rings (zone). Along this zone, most of the agricultural areas, village buildings, and concrete walls of the village cemetery were damaged. These earth fissures are associated with ground subsidence in some

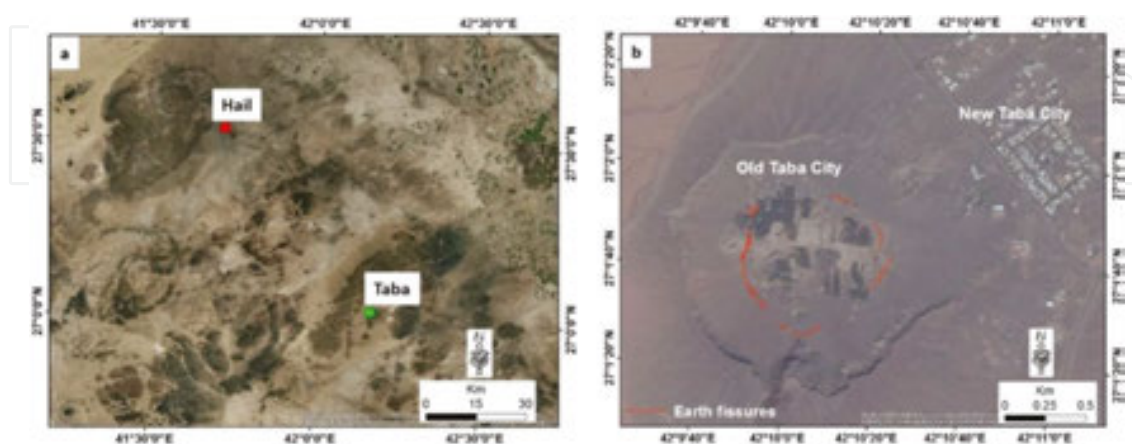


Figure 2. (a) Location of Tabah village related to the Hail city; (b) Location of earth fissures in the old Tabah village in relation to the New Tabah village.

parts, showing a vertical displacement (up to 1.5 m). We believe that these earth fissures and ground subsidence are not yet completed and will continue in the future.



Figure 3. Photographic pictures showing (a) Earth fissures' distribution, (b) Impact of earth fissures on buildings.

2.3.2. Topography and geology

Analysis of satellite image and topographic map of the study area indicated that the earth fissures are located between elevations of 1020 m and 1030 m from the mean sea level. Geologically, the study area consists of the following geological units from the youngest to the oldest as follows (**Figure 4**): (1) Khabra deposits (Qk), including silt, clay, and some sand; (2) Reworked volcanic ash deposit (Qa) consisting of a redeposition of ancient volcanic deposits;

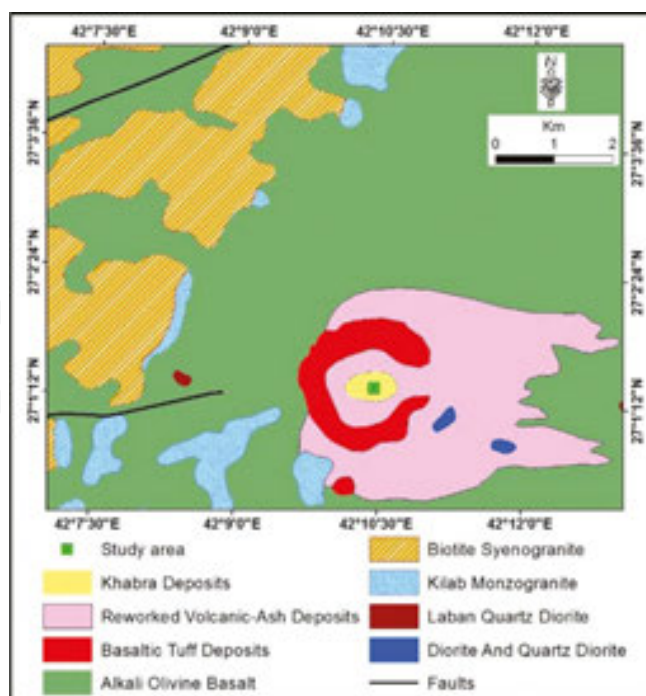


Figure 4. Surface geological map of the study area and its surrounding.

(3) Basaltic tuff deposit (Qt); (4) Alkali olivine basaltic rocks (Qb); (5) Biotite syenogranite rocks (sgb); (6) Kilab mozogranite rocks (kmg); (7) Laban quartz diorite rocks (lqd); and (8) Diorite and quartz diorite rocks (di).

2.3.3. Geophysical investigation and analysis

Geophysical investigation using the electrical-resistivity method was performed and is presented in this chapter. Electrical-resistivity tomography (ERT) represents commonly used geophysical techniques for the detection of earth fissures, which has been widely used in the KSA, producing satisfactory results. ERT is particularly useful in areas with significant resistivity contrasts. For measurements, four electrical-resistivity lines were performed in the old Tabah village (**Figure 5**). The first electrical line has a west-to-east direction with a total length of 285 m and spacing of 1 m and 3 m between electrodes, while the remaining three lines have south-to-north direction and lengths of 960 m, 470 m, and 470 m for the second, third, and fourth lines, respectively. The spacing between the electrical poles is 10 m each.

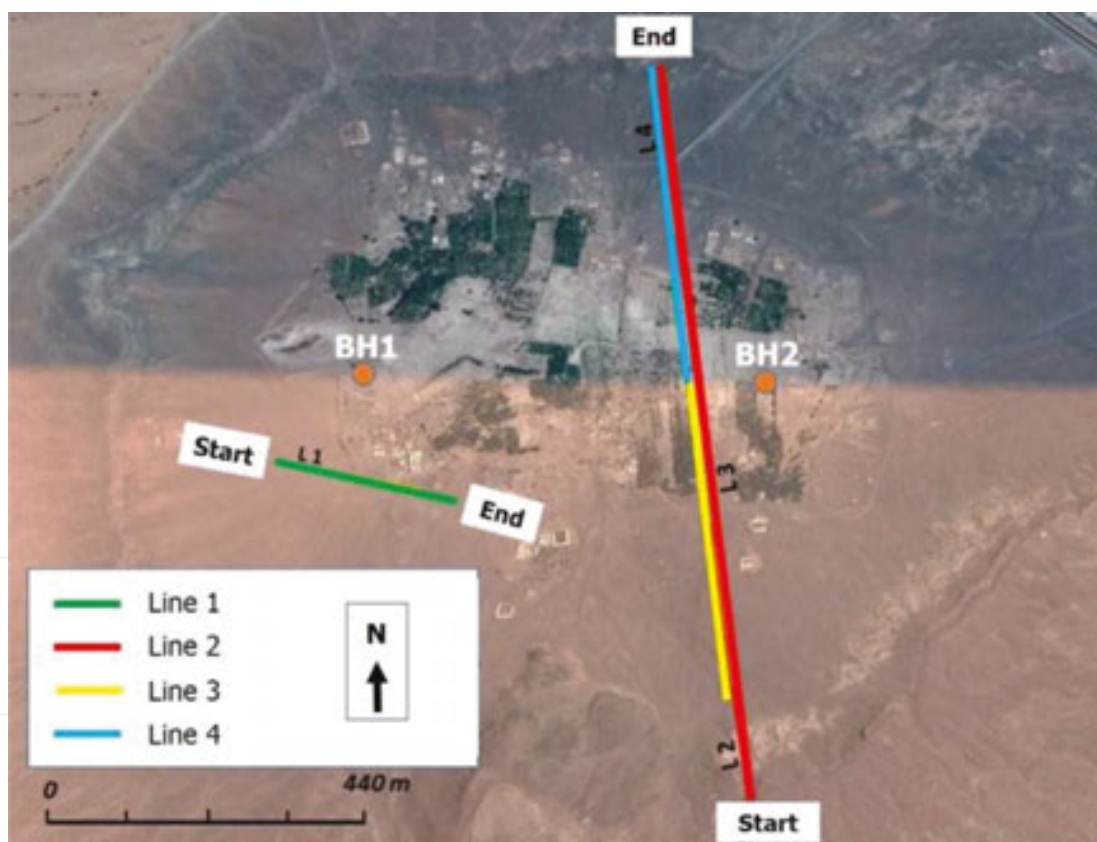


Figure 5. Distribution of geophysical lines and boreholes in the study area.

Line 1 (L1) moves across the earth fissures with a west-to-east direction. It applied with 1 m electrode spacing (**Figure 6a**) and 3 m spacing (**Figure 6b**). Information collected using this line shows that the soil in the region, which consists of Quaternary and volcanic ash sediments, has low electrical resistance up to the maximum depth of the profile (40 m). The decrease in

the electrical resistance values is related to the water-saturation effect. It reveals the presence of vertical fissures in the middle part of the electric line (L1) (**Figures 6a, b**), which represents the contact line between the water-saturated soil and the Precambrian complex rocks, which has high electrical resistance. These hard rocks begin from 5 m under the surface and extending up to 40 m deep.

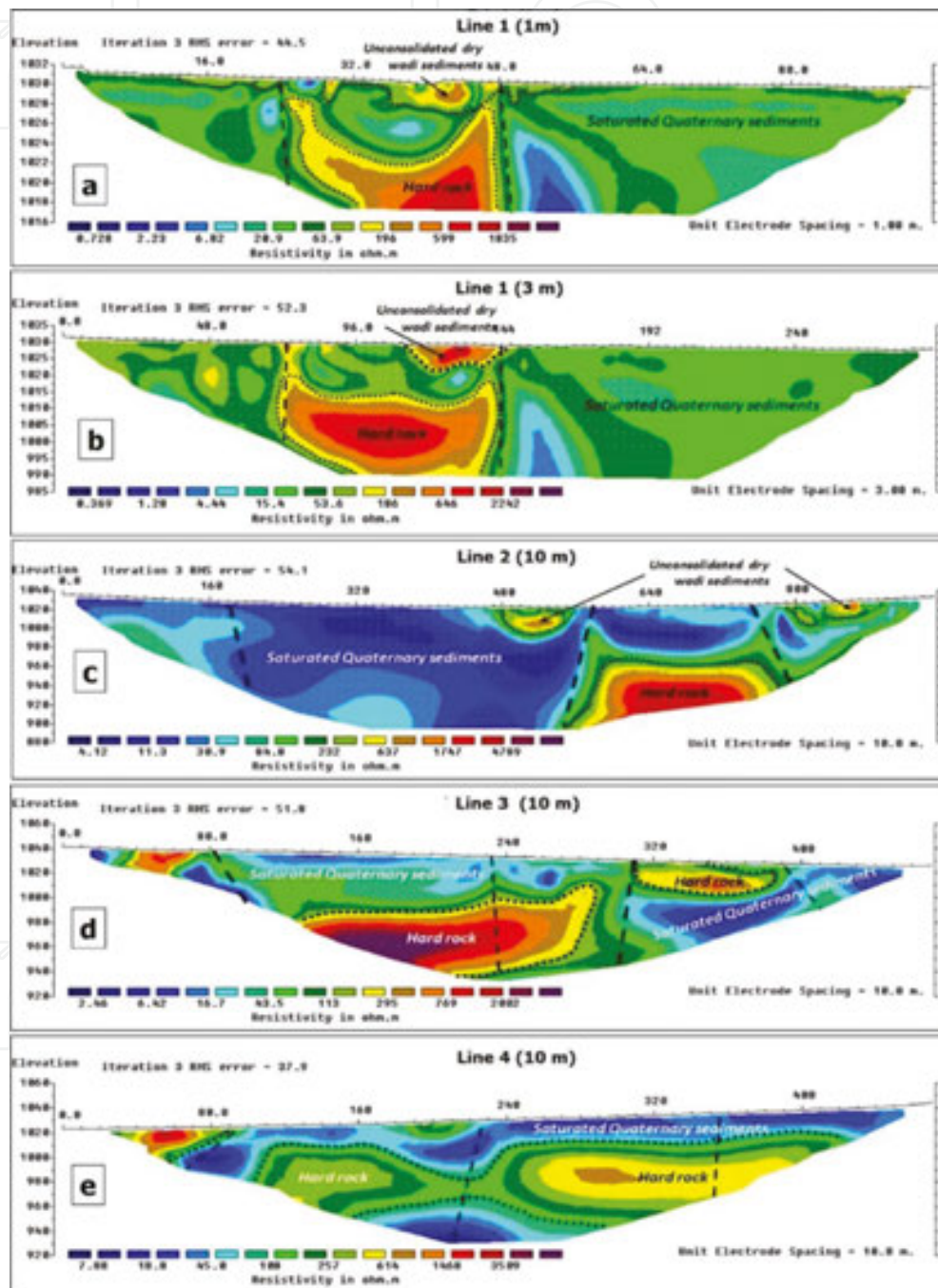


Figure 6. Electrical-resistivity profiles of different lines:(a) Line 1 with 1 m electrode spacing; (b) Line 1 with 3 m electrode spacing; (c) Line 2 with 10 m electrode spacing; (d) Line 3 with 10 m electrode spacing; and (e) Line 4 with 10 m electrode spacing. Note: horizontal axes do not have the same scale.

Line 2 (L2) moves across the earth fissures with a south-to-north direction with a total length of 950 m, 10 m electrode spacing, and reaches up to 130 m depth (**Figure 6c**). It is clear that there is a large underground reservoir with a large thickness as the electrical resistance values are low. The end of the profile shows the presence of high-resistance materials (solid rocks) at a depth of 50 m, extending beyond the total depth of the profile (130 m deep). Different deep earth fissures were detected along the profile and appeared at the contact between sediments and hard rocks (**Figure 6c**).

Line 3 (L3) moves across the earth fissures with a south-to-north direction with a total length of 470 m, and 10 m electrode spacing (**Figure 6d**). It was found that this profile reflects the same phenomena that have been monitored in Lines 1 and 2 where there is a large zone of water-saturated sediments (with low electric resistance), which intruded with hard rocks (with high electric resistance). The hard rocks appear at a depth between 30 m and 50 m in the middle of the profile. Various deep earth fissures were detected along the profile at distances of 80 m, 230 m, 310 m, and 390 m from the start point of the line (**Figure 6d**). These earth fissures mostly appear along the contact between soil and rocks.

Line 4 (L4) moves across the earth fissures with a south-to-north direction with a total length of 470 m and 10 m electrode spacing (**Figure 6e**). It was found that this profile reflects the same phenomena that have been monitored in Lines 1, 2, and 3 where there is a large zone of water-saturated sediments (with a low electric resistance), which intruded with hard rocks (with high electric resistance). Hard rocks appear as a horizontal layer at a depth of 10 m from the surface. Various deep earth fissures were detected along this profile (L4) at distances of 100 m, 210 m, and 345 m from the start point (**Figure 6e**). These earth fissures mostly appear along the contact between soil and rocks.

2.3.4. Geotechnical investigation and analysis

Two boreholes were drilled in the study area to investigate the subsurface soils and rocks (**Figure 5**). Analysis of the boreholes indicated that the sediment layer is characterized by alternation of sand with silt, clay with silt, sand with clay, and silt and some gravels and different rocks (**Figure 7**). These deposits have color ranging from light brown to brown and a thickness of 19 m (BH 1) to 144 m (BH 2). According to the unified soil classification system (USCS), these sediments include (a) clay with silt (CL–ML), which are characterized by liquidity-limit values ranging 18–28, plastic-limit values ranging 12–21, and plastic-index values ranging 5–7; (b) sand with silt (SM) and sand with silt and clay (SC–SM), which are characterized by a liquidity-limit value of 13, plastic-limit value of 9, and a plastic index value of 4.

Rocks are characterized by the following: (a) clay stone is characterized by gray to white color, includes some clay and silt, highly fractured, the rock-quality designation (RQD) ranging from very poor to poor (0–40) percent of the recovery ranging from 40 to 100%, and the uniaxial compressive strength ranging from 0 MPa to 4.3 MPa; (b) sandstone is characterized by brown color, highly fractured, the rock-quality designation (RQD) ranging from very poor to fair (20–66), the recovery percent of 100%, and the uniaxial compressive strength ranging from 4.6 MPa to 7.4 MPa; (c) siltstone is characterized by brown color, moderately to highly fractured, the

rock-quality designation (RQD) ranging from very poor to fair (0–40), the recovery percent ranging from 90 to 100%, and the uniaxial compressive strength ranges from 1.4 MPa to 7.2 MPa; (d) igneous rock is characterized by brown color, fine grained, slightly to highly fractured, the rock-quality designation (RQD) ranging from very poor to fair (0–74), the recovery percent of 100%, and the uniaxial compressive strength ranging from 1.1 MPa to 15.3 MPa.

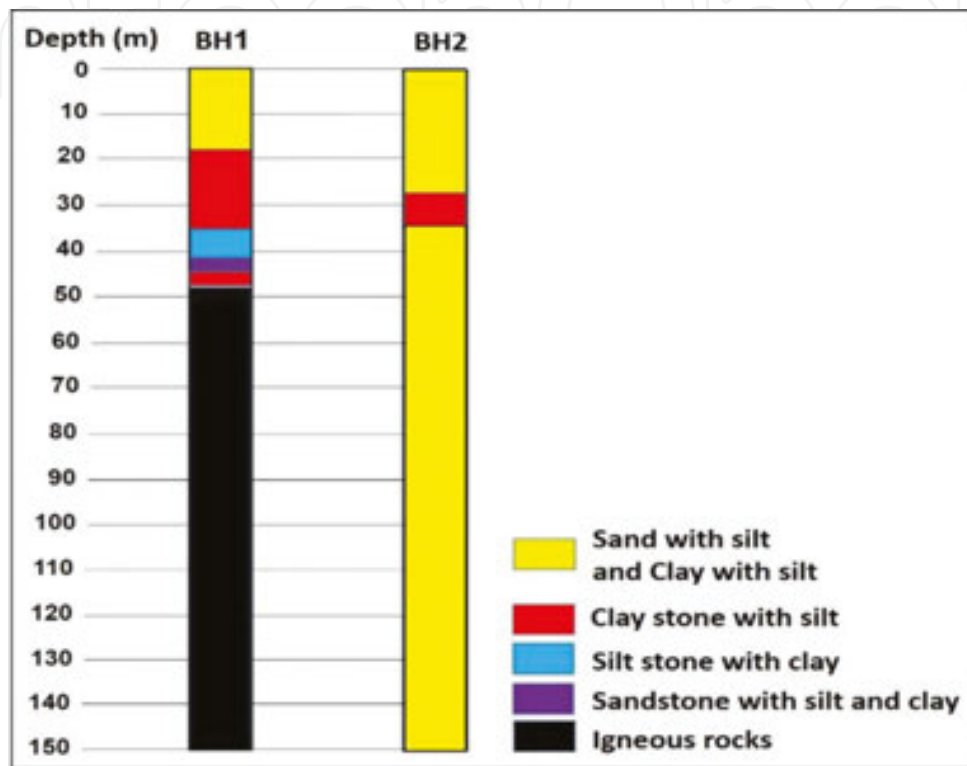


Figure 7. Lithology of boreholes.

2.3.5. Causes of earth fissures

Throughout the abovementioned field, remote-sensing maps, geological, geophysical, and geotechnical investigations and analysis, the earth fissures and ground subsidence in Tabah area have been observed to be occurring since many decades ago and still continuing. The study indicated that these earth fissures were located inside the volcanic crater, which was deep and open. The volcanic tuffs and agglomerate surrounding the vent were eroded due to the effect of rainfall and filled the vent. These earth fissures are related to the development of agricultural activities, which mainly depend on groundwater withdrawal. Most causes of earth fissures can be discussed as follows:

- a. The area is characterized by the presence of agricultural areas since few decades ago, which mainly depend on the groundwater aquifer in the area (Figure 8). According to the information obtained from residents of the area, the groundwater level was near the earth's surface (<50 m below the surface) 30 years ago. As a result of drilling of a large number

of groundwater wells (for domestic use, irrigation, and road building, which in turn led to extensive withdrawal of huge amounts of groundwater), the water level declined to the level of 120 m in 1985 and now lower than 160 m below the earth's surface.

- b. Subsurface materials in the Tabah area is characterized by breccia, gravel, sand, silt, and clay as well as different rocks such as claystone, siltstone, and sandstone. The sediments extend to a depth greater than 150 m at Borehole 2 and may increase in the middle of the area. The thickness of these sediments decreased outwards to about 48 m in Borehole 1 and decreased outwards until igneous rocks appear on the surface.
- c. As a result of the topography irregularity, the thickness of the sediments increased toward the centre of the area and decreased outwards where the solid rocks become near the surface especially on the sides of the area. As a result of the groundwater withdrawal, the water level significantly declined, leading to the compression of the sediments. According to the differential settlement of these sediments, along the edges, the amount of settlement is small and increases toward the centre of the area. This leads to the appearance of earth fissures at the contact surface between hard rocks and deep sediments. Some of these fissures have vertical displacement. **Figure 9** shows a model for the earth-fissure development. The geophysical and geotechnical investigations confirmed this theory as the cause of earth fissures.

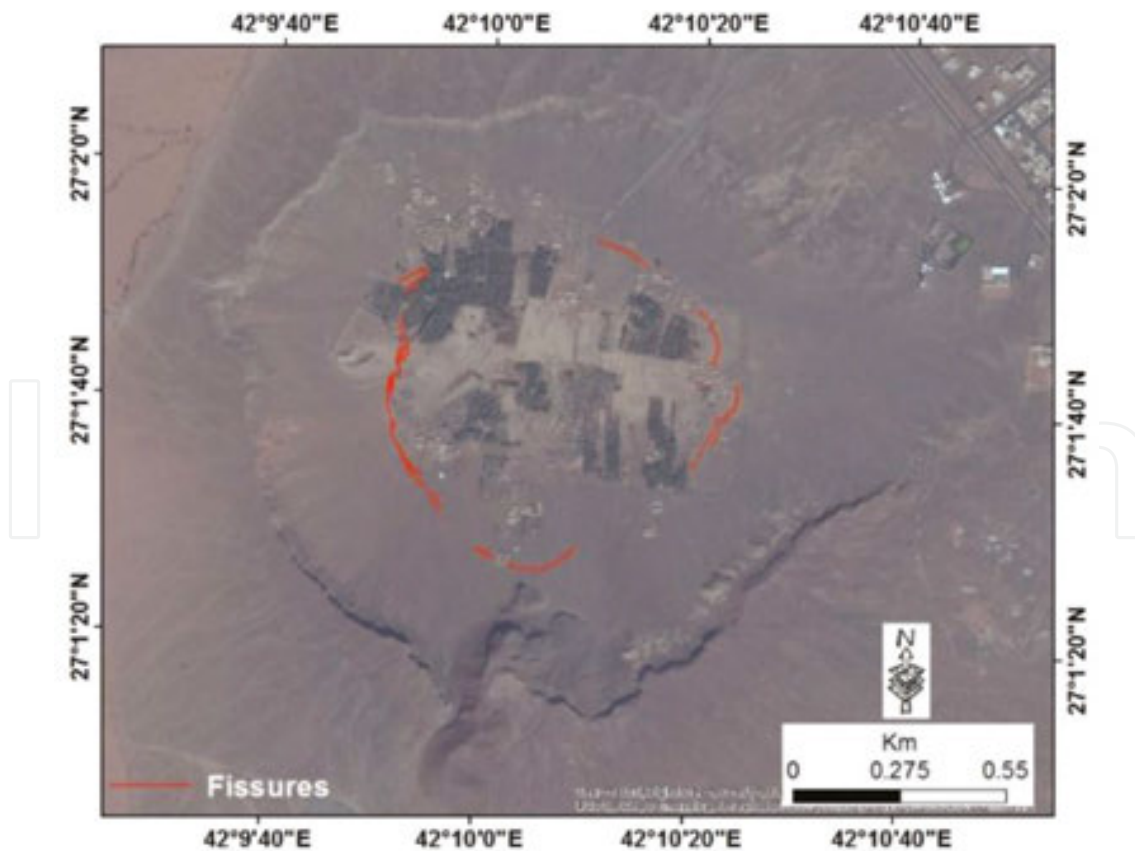


Figure 8. An example of agricultural activities in Tabah area.

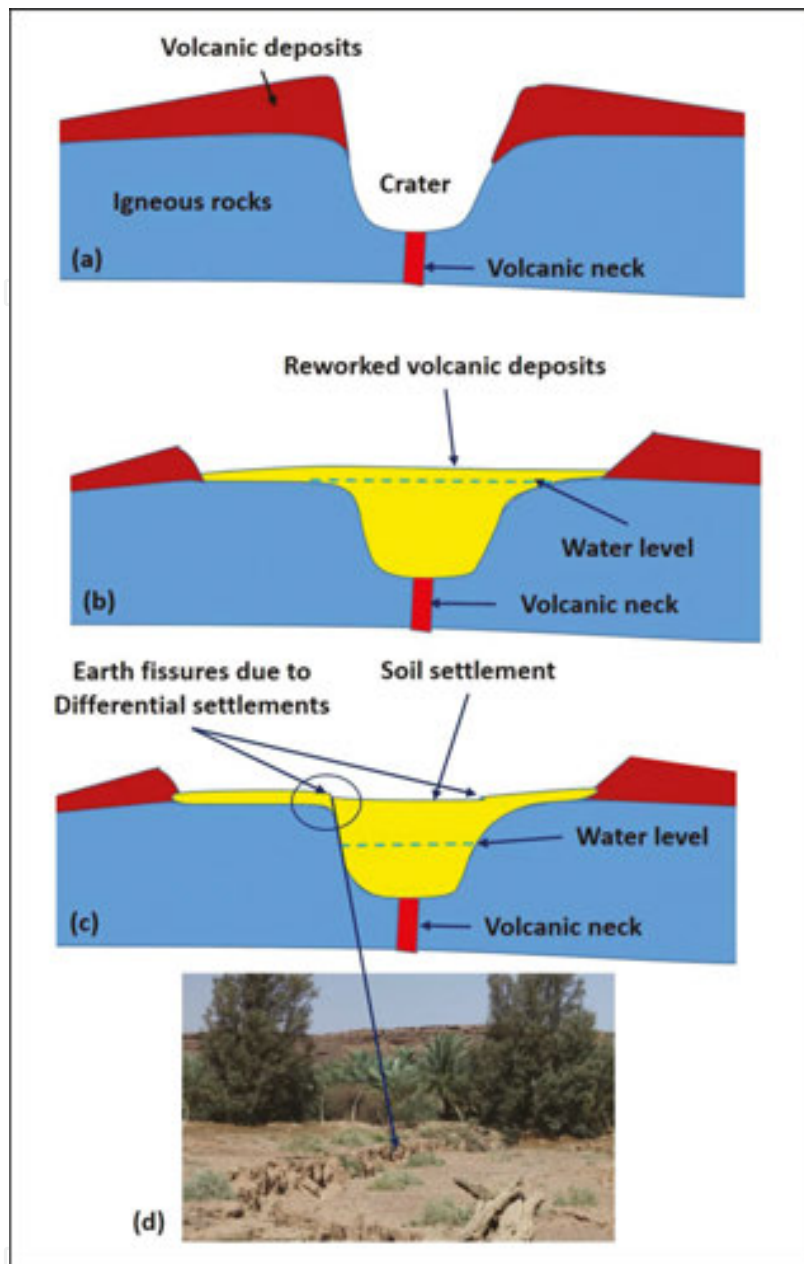


Figure 9. Earth fissure development model in Tabah area (modified after Roobol et al. [24]): (a) Before erosion of volcanic deposits; (b) After erosion of volcanic deposits and refill, the vent, water table is very shallow; (c) Current condition, water table ~160 m deep and earth fissures occurred; and (d) Photograph showing current earth fissures.

3. Case-study group 2: sinkholes induced by human activities in the KSA

3.1. Karst backgrounds

Karstic rocks cover a large area of the Kingdom of Saudi Arabia, mainly in the eastern and northern parts [44]. Sinkholes, the main manifestation of Karstification on ground surface,

represent one of the natural geohazards. Most damaging incidents related to the presence of sinkholes are induced by human activities. Many cases in the KSA illustrate that there is increasing human impact on the natural environment and aquifers due to the rise in human development and activity. Interstratal dissolution of these formations and the subsidence of the overlying sediments has generated numerous large subsidence depressions and sinkholes [16, 45, 46]. In fact, Ar Riyadh, the capital of the Kingdom, is located on a large inactive subsidence depression related to interstratal evaporite dissolution [46–48]. A similar situation is found in other sectors of the country underlain by the Late Cretaceous Badanah and Zallum formations with interbedded evaporites at shallow depth [49]. Here, extensive tracts are riddled by khabras that correspond to subsidence depressions generated by interstratal karstification of evaporites and the subsidence of overlying sediments [50]. Youssef et al. [10] indicated that a large number of new sinkholes have been discovered in recent years, notably in Ar Riyadh area, the Al Summan Plateau northeast of Ar Riyadh, in an extensive belt south of Ar Riyadh extending as far as Sulayyil, in the eastern and northern provinces, and in Jazan area on the western coast. They indicated that most of the recently documented sinkholes are related to human activities that may cause dissolution and/or subsidence processes (groundwater withdrawal, irrigation, water leakage, and overloading), suggesting a significant induced component. Various types of sinkholes were recorded in the KSA that are related to human activities [10]. These sinkholes were categorized based on the classification presented by Gutiérrez et al. [51–53]. Gutiérrez et al. [51–53] classified sinkholes into two types: solution sinkholes and subsidence sinkholes. They indicated that (1) solution sinkholes are shallow, enclosed depressions generated by differential lowering of the surface in karstic rocks; and (2) subsidence sinkholes are resulting from subsurface dissolution and downward gravitational movement of the materials. The subsidence sinkholes in the adapted classification use two terms: one related to material affected by subsidence (cover, bedrock, and caprock), and the second term represents the subsidence mechanism (collapse, suffosion, and sagging). In the KSA, different types of subsidence sinkholes were recorded including cover- and caprock-collapse sinkholes, cover-suffosion sinkholes, sagging sinkholes, and complex sinkholes. Cover refers to unconsolidated deposits; caprock refers to nonkarstic rocks; collapse indicates the brittle deformation of soil or rock material; suffosion is the downward migration of unconsolidated cover deposits through conduits; and sagging is the downward bending of ductile sediments. Complex sinkholes, on the other hand, involve more than one material type and different subsidence mechanisms. In the current section, different examples of these sinkholes in the KSA will be discussed in detailed:

1. Cover-collapse sinkholes case study, Al Jouf farm sinkhole: this type of sinkhole is a cover collapse sinkhole, located at a latitude of $29^{\circ}46'43.68''\text{N}$. and longitude of $38^{\circ}27'37.02''\text{E}$. This sinkhole has 40 m diameter and 15 m depth. It occurred in 2006 within a farm circle (**Figure 10a**). Geologically, the limestone bedrock of the Sirhan formation is overlain by a thick Quaternary cover (Aeolian sands capped by a quartz-rich gravel sediments). This sinkhole is formed due to excessive groundwater extraction, which started in 1989. Recent measurements of the water table indicated that the water level is at about 205 m deep from the ground surface. The drawdown of the water table has reached ~100 m.

2. Caprock-collapse sinkhole case study, Al Issawiah sinkholes: four sinkholes were recognized in Al Issawiah area, and some of them are caprock-collapse sinkholes. One of them is located at a latitude of $30^{\circ}43'30.5''\text{N}$. and longitude of $38^{\circ}06'01''\text{E}$. It is a subcircular collapse sinkhole with a diameter of 27 m and a depth of 23 m. It is opened on a basaltic caprock (**Figure 10b**). Geologically, the Sirhan formation in this area consists of friable calcareous sandstone, limestone, and shale, unconformably overlain in some areas by basalt of the Harrat Al Harrah lava field [54]. The basalt is covered by a thin silty soil plus discontinuous sand dunes and residual basalt boulders. In other areas, the basaltic layer disappears (**Figure 10c**). Field investigations indicated that the water table was exposed at the bottom of the sinkhole; with increasing groundwater exploitation because of increasing irrigation crops, the depression became dry and the water table declined.
3. Cover-suffosion sinkholes: cover-suffosion sinkholes develop in areas with karstified bedrock covered by an unconsolidated soil. These cover deposits may migrate downward through dissolutional conduits and enlarged joints. This leads to the progressive settlement of the ground surface. This type of sinkhole was recorded in Al Khafji area with a diameter of 70 m (**Figure 10d**). Geologically, the area consists of limestone-bearing bedrock of the Hadruk formation overlain by a thick low-cohesion sand-gravel cover. This type is characterized by an ellipsoidal depression, 520 m long and 310 m wide. This sinkhole was potentially triggered because of lowering of the water table due to groundwater pumping from the Hadruk formation and the underlying Dammam karst aquifer.
4. Sagging sinkholes: sagging sinkholes involve the progressive passive bending of sediments related to dissolution of underlying soluble material. This type of sinkholes appears in many areas in the KSA, which are underlain by various formations such as Jilh, Arab, Zallum, Badanah, and Umm er Radhuma formations. Most of these areas are characterized by khabras deposits, which are filled by Quaternary fine-grained deposits. Many authors indicated that these khabras correspond to large sagging sinkholes relating to differential, interstratal karstification of the gypsum beds and the progressive ductile bending of the overlying rock strata [47, 49, 50, 55]. Another example of sagging sinkholes was documented in the sabkha environment in Jizan area where there was subsurface dissolution of evaporites, frequently induced by artificial water input into the ground and caused ground settlement (**Figure 10e**) [1].
5. Complex sinkholes: these types of sinkholes result from the combination of two subsidence mechanisms (sagging and collapse processes). Many examples were documented in different areas of the KSA, including:
 - a. Aba Alwrood sinkhole located in Al Qasim Region at the latitude of $26^{\circ}25'52.16''\text{N}$. and longitude of $44^{\circ}03'10.69''\text{E}$. This sinkhole is a sagging and collapsing sinkhole which is 10.5 m long and 7.5 m wide that occurred in 2010 (**Figure 10f**). Geologically, the gypsum bedrock is of Jilh Formation of Triassic-age [56].
 - b. Turaif sinkhole is located in Al Qasim Region, at the latitude of $26^{\circ}49'26.65''\text{N}$. and longitude of $44^{\circ}09'46.83''\text{E}$. Geologically, this sinkhole area consists of thinly bedded gypsum, limestone, and shale of the Triassic Jilh Formation [56]. The layers in the sinkhole

display downward bending, indicating two mechanisms of subsidence, including sagging and collapsing (**Figure 10g**).

- c. Bsita sinkhole is located in Al Jouf Region, at the latitude of $30^{\circ}11'16.8''\text{N}$. and longitude of $37^{\circ}51'1.88''\text{E}$. This sinkhole has an oval shape with a length of 100 m and width of 60 m (**Figure 10h**). Geologically, Palaeocene- and Eocene-age rocks of Mira formation are exposed in the area. These rocks consist of a thinly bedded silicified limestone and banded chert [54]. The studied evidence of this sinkhole indicates that the depression corresponds to a sagging-collapse sinkhole [10].



Figure 10. (a) Cover-collapse sinkhole in Al Jouf farm company area; (b) Caprock-collapse sinkhole in Al Issawiah area; (c) Caprock-collapse sinkhole in Al Issawiah area; (d) cover-suffosion sinkhole in Al Khafji area; (e) sagging sinkhole in Jizan area; (f) Bedrock-collapse and sagging sinkhole in Aba Alwrood area, Al Qasim region; (g) Bedrock-collapse and sagging sinkhole in Turaif area, Al Qasim Region; and (h) Bedrock sagging and collapse sinkhole at Bsita, Al Jouf Region.

3.2. Methods of sinkhole investigations

3.2.1. Using geologic and topographic maps

The Kingdom of Saudi Arabia is located on the southern part of the Arabian Plate. According to the geological maps of 1:250,000 scale, which covers the KSA, an important information on the distribution of different rock units can be obtained as shown in (Figure 11). The KSA consists of three main geological zones:

Zone 1: The Arabian Shield, situated on the western part of the KSA. It consists of Precambrian rocks, locally covered by Cenozoic lava flows [57].

Zone 2: The Arabian Platform, situated on the eastern and northern part of the KSA. It is characterized by a Phanerozoic sedimentary succession [58]. It includes a significant proportion of carbonate and evaporite karst formations.

Zone 3: The Quaternary sediments cover a narrow coastal strip along the margin of the Red Sea and the east margin of the KSA. It also covers some areas of Zone 2. According to this map, it was found that the carbonate and evaporate rocks cover a significant portion of the KSA, which is exposed on the surface and sometimes covered by other rock formations. Different types of sinkholes were documented and mapped along Zone 2 [41–43, 46, 49, 59–62].

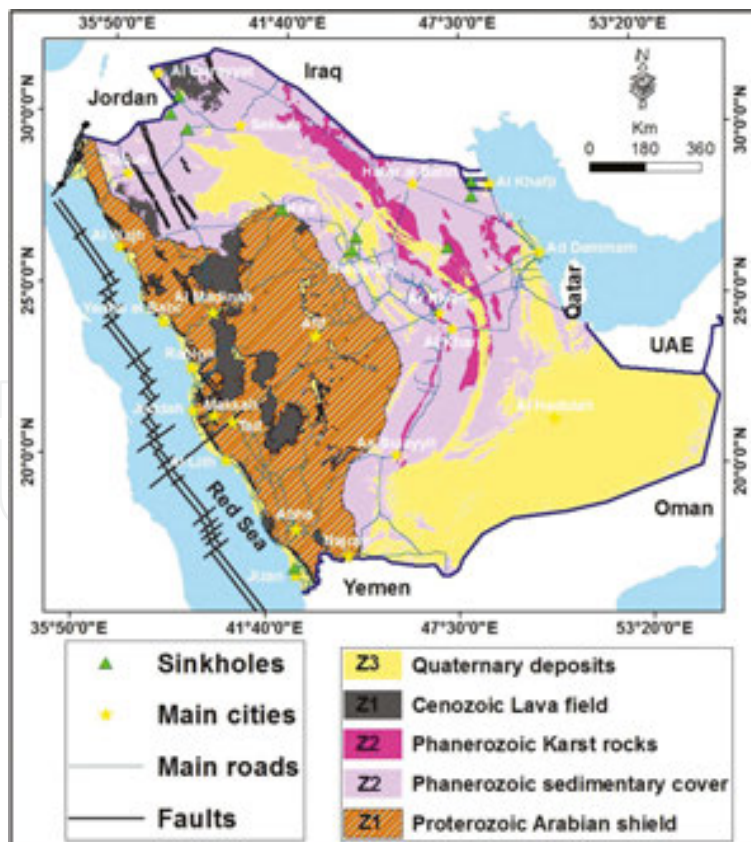


Figure 11. Geological map of the KSA showing areas of earth fissures and sinkholes.

According to topographic maps of 1:50,000 scale, different types of depressions related to dissolutions were detected and mapped. These depressions have local names (Dahls). The presence of these depressions can give a good indication of the presence of sinkholes and dissolution-induced subsidence depressions. Many studies were conducted on these depressions that are mapped in the topographic maps, and they verified that these depressions are related to dissolution and collapse sinkholes [10]. Some of these depressions (Dahls) on a topographic map of An Nu'ayriyah area is shown in **Figure 12**.

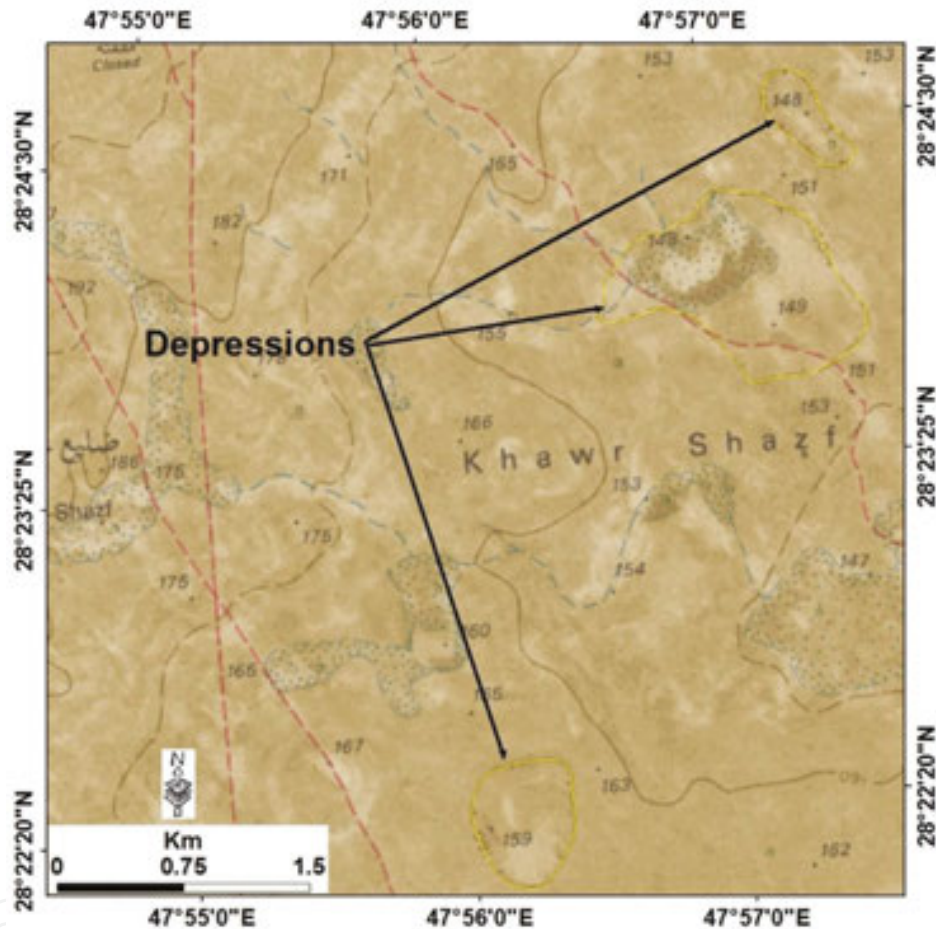


Figure 12. Topographic map of a small part of An Nu'ayriyah area showing dahls (potentially sinkhole areas).

3.2.2. Using remote-sensing images

One of the popular, nondestructive methods for detecting karst-related features and sinkholes is the use of remote-sensing data. These remote-sensing data can be used for recognizing different surface features that are related to karst phenomena using visual inspection. Different types of remote-sensing data have previously been used for distribution and recognition of sinkholes and karst-surface features such as aerial photographs [63, 64] and satellite images [10, 17]. In the KSA, aerial photographs are very rarely and in a limited manner used for detecting karst related features. However, Landsat images of 15 m resolution can easily be

prepared using the fusing technique to sharpen the resolution of 30 m bands 1, 2, 3, 4, 5, and 7 to enhance the resolution to 15 m resolution using panchromatic band 8. These data were used before to detect surface features (circular features, depressions, and ring structures) that are related to karstification at An Nu'ayriyah area (**Figures 13a, b**). Another set of remote-sensing data was used to detect sinkholes, including the imagery of professional Google Earth. These high-resolution images were used in different projects in the KSA and give valuable information about the presence of sinkholes and their time of occurrence. **Figures 13c, d** shows some examples of Google Earth high-resolution images with different sinkholes at Al Issawiah area.

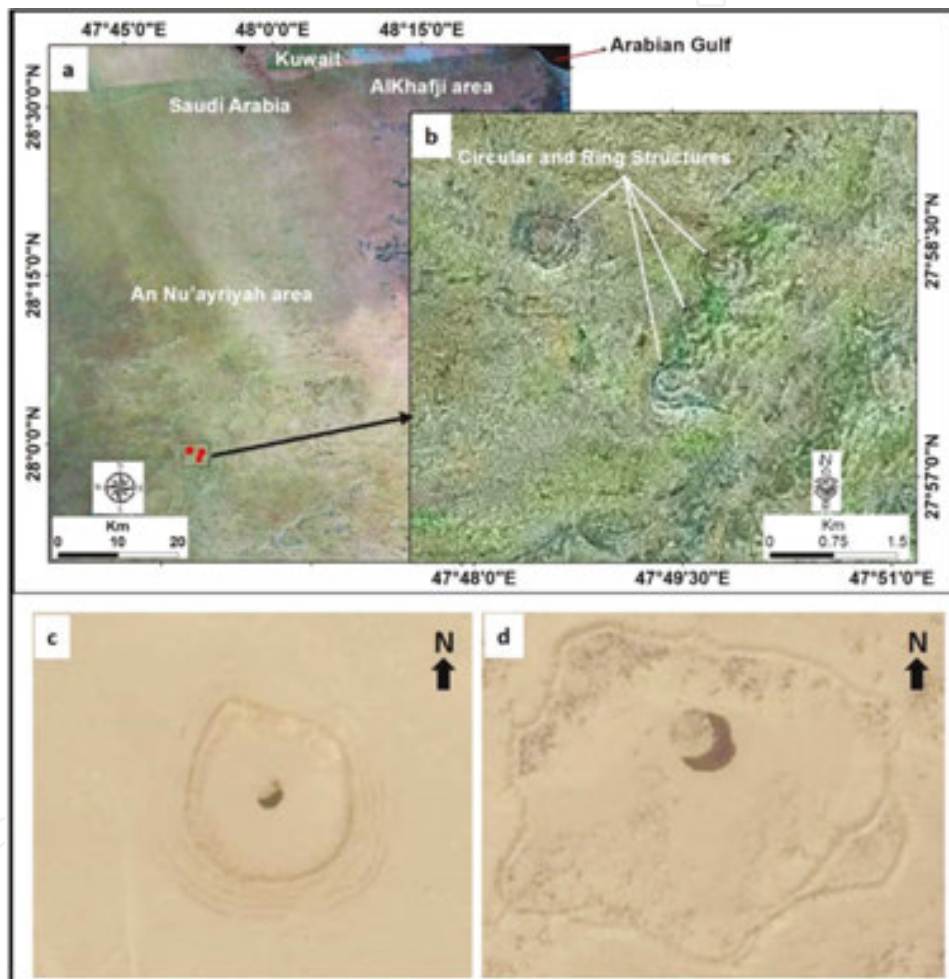


Figure 13. (a) Circular and ring structure features at An Nu'ayriyah area;(b) Circular and ring structure features at An Nu'ayriyah area; (c) Google-earth map of sinkholes at Al Issawiah area; (d) Google-earth map of sinkholes at Al Issawiah area.

3.2.3. Field investigation using trenching technique and borehole technique

The trenching technique has previously been applied in different investigations by many authors [10, 63, 65–68]. The trenching method depends on the excavation of trenches at the

study site, mapping the exposed stratigraphy and structure as well as reconstructing the deformation history. The trenching technique has been applied in different fields such as ground instability (landslides) and sinkholes. Many examples were performed in the KSA to investigate the cover-collapse sinkholes. The trench has to be excavated perpendicularly to the edge of the sinkhole. Youssef et al. [10] mentioned that the walls of the trench must be cleaned and, then, logged on graph papers at a rescannable scale using an orthogonal grid of strings with a spacing of 1 m. Trenching method has various aims, including: (a) internal structure and subsidence mechanisms investigation (deformation style); (b) checking whether the sinkhole was an incipient-collapse feature or the reactivation of a pre-existing buried collapse depression; and (c) reconstructing the evolution of this presumably human-induced sinkhole to build a prognostic basis.

3.2.4. Detection of subsurface-karst features using geophysical techniques

Electrical-resistivity tomography technique is one of the most commonly used geophysical methods for the detection of cavities and buried sinkholes in karstic regions. This method depends on imaging the subsurface materials (according to the bulk electrical resistivity of each material type) by multielectrode systems [69]. Electrical-resistivity tomography (ERT) method gives excellent results in areas with significant electrical-resistivity contrasts. This is expected to occur in karstic terrains where most cavities, with considerable sizes, are filled with low electrical-resistivity deposits [10, 17, 18, 68, 70–74]. The electrical-resistivity tomography (ERT) is very common in the KSA, and reasonable results could be obtained using this method [11, 17, 18]. Electrical-resistivity and seismic techniques have been applied in different areas in the KSA and have been successful detecting sinkholes [10, 17, 75].

3.3. Causes of sinkholes

All sinkholes in the KSA are formed according to the presence of underlain cavernous limestone and evaporites. Formation of these sinkholes could be explained as subsidence and collapse processes that occurred above old cavities, probably formed during past pluvial phases. Gutiérrez et al. [53] and Youssef et al. [10] indicated that sinkhole-formation mechanisms can easily be initiated and accelerated by human activities (groundwater withdrawal, irrigation, and overloading). According to the available information of the sinkholes in the KSA, there are different anthropogenic factors that trigger the formation of sinkholes development including:

1. Excessive groundwater pumping from limestone-formation aquifers: this leads to rapid water-table decline and loss of buoyant support in the roof of pre-existing cavities and an increase in the effective stress. In addition, internal erosion processes could happen due to decline of water table. Different types of sinkholes have been recently recorded under this type of scenario, especially in the northern and central areas of the KSA (Al Jouf and Al Qasim Regions).
2. Dissolution of salt rocks and deposits due to infiltration of freshwater (leaking pipes) into the subsurface salt rocks and deposits: this process has been documented in Jazan area

where the old Jazan city was built on a salt dome and on the adjacent sabkha areas. The entire old Jazan city has been abandoned due to the severe damage by subsidence [1]. Irrigation and rainwater infiltration: this leads to an increase in the top-soil unit weight and a decrease in its strength and cohesion (silt and clay materials). That leads to a migration of cover deposits through underlying cavities.

3. Loading and man-made vibrations (static and dynamic loads): these lead to the collapse of unstable cavities. Many examples were documented in the KSA such as the sinkhole at Al Khobar city, in the eastern province, induced by the load of a vehicle on a road.
4. Excavation: This leads to the surface appearance of cavities underneath. One example of the appearance of underground cavities was reported during the construction of the wastewater treatment system in Ar Riyadh city where there are Arab, Hith, and Sulaiy formations (limestone and anhydrite).

Author details

Ahmed M. Youssef^{1,2*}, Hasan M. Al-Harbi¹, Yasser A. Zabramwi¹ and Bosy A. El-Haddad²

*Address all correspondence to: amyoussef70@yahoo.com

1 Geological Hazards Department, Applied Geology Sector, Saudi Geological Survey, Jeddah, Kingdom of Saudi Arabia

2 Geology Department, Faculty of Science, Sohag University, Egypt

References

- [1] Youssef AM, Pradhan B, Sabtan AA, El-Harbi HM. (2011) Coupling of remote sensing data aided with field investigations for geological hazards assessment in Jazan area, Kingdom of Saudi Arabia, *Environmental Earth Sciences*, 65(1):119–130. Doi: 10.1007/s12665-011-1071-3.
- [2] Crawford NC. (1984) Sinkhole flooding associated with urban development upon karst terrain: Bowling Green, Kentucky. In *Proceedings of the First Multidisciplinary Conference on Sinkholes*, ed. Beck BF, Balkema AA. Rotterdam. pp. 283–292.
- [3] Gao Y, Luo W, Jiang X, Lei M, Dai J. (2013) Investigations of large scale sinkhole collapses, Laibin, Guangxi, China. In: LandL, Doctor, DH, Stephenson, JB (Eds). *Sinkholes and the Engineering and Environmental Impacts of Karst*. National Cave and Karst Research Institute. pp. 327–331. Carlsbad, NM: The National Cave and Karst Research Institute (NCKRI). www.karstportal.org/sites/karstportal.org/files/KIP-00011836.pdf

- [4] Gutiérrez F. (2010) Hazards associated with karst. In: Alcántara I and Goudie A. (Eds.). *Geomorphological Hazards and Disaster Prevention*. Cambridge University Press. Cambridge. pp. 161–175.
- [5] Gutiérrez F. Mozafari M. Carbonel D. Gómez R. Raeisi E. (2014a) Leakage problems in dams built on evaporites. The case of La Loteta Dam (NE Spain), a reservoir in a large karstic depression generated by interstratal salt dissolution. *Engineering Geology*, 185:139–154.
- [6] Li J. Zhou W. (1999) Subsidence in karst mining areas in China and some methods of prevention. *Engineering Geology*, 52:45–50.
- [7] Milanovic PT. (2000) *Geological Engineering in Karst*. Zebra, Belgrade. 347 pp.
- [8] Song KI. Cho GC. Chang SB. (2012) Identification, remediation and analysis of karst sinkholes in the longest railroad tunnel in South Korea. *Engineering Geology*, 135–136:92–105.
- [9] Waltham T. Bell F. Culshaw M. (2005) *Sinkholes and Subsidence: Karst and Cavernous Rock in Engineering and Construction*. Springer, Berlin. 382 pp.
- [10] Youssef AM. Al-Harbi HM. Gutiérrez F. Zabramwi YA. Bulkhi AB. Zahrani SA. Bahamil AM. Zahrani AJ. Otaibi ZA. El-Haddad BA. (2016) Natural and human-induced sinkhole hazards in Saudi Arabia: distribution, investigation, causes and impacts. *Hydrogeology Journal*, 24(3):625–644. DOI: 10.1007/s10040-015-1336-0.
- [11] Abdeltawab S. (2013) Karst limestone foundation geotechnical problems, detection and treatment: Case studies from Egypt and Saudi Arabia. *International Journal of Scientific & Engineering Research*, 4:376–387.
- [12] Amin A. Bankher K. (1997a) Karst hazard assessment of Eastern Saudi Arabia. *Natural Hazards*, 15:21–30.
- [13] Amin A. Bankher K. (1997b) Causes of land subsidence in the Kingdom of Saudi Arabia. *Natural Hazards*, 16:57–63.
- [14] Edgell HS. (1990) Karst in northeastern Saudi Arabia. *Journal of King Abdulaziz University, Earth Sciences*, 3:81–94.
- [15] Erol AO. (1989) Engineering geological considerations in a salt dome region surrounded by sabkha sediments, Saudi Arabia. *Engineering Geology*, 26:215–232.
- [16] Kempe S. Dirks H. (2008) Layla Lakes, Saudi Arabia: The world-wide largest lacustrine gypsum tufas. *Acta Carsologica*, 37(1):1–14.
- [17] Youssef AM. Al-Qaluobi H. Zabramawi YA. (2012a) Integration of remote sensing and electrical resistivity methods in sinkhole investigation in Saudi Arabia. *Journal of Applied Geophysics*, 87:28–39. Doi: 10.1016/j.jappgeo.2012.09.001.

- [18] Youssef AM. Al-Qaluobi H. Zabramawi YA. (2012b) Sinkholes detection using electrical resistivity tomography (ERT) in Saudi Arabia. *Journal of Geophysics and Engineering*, 9:655–663. Doi: 10.1088/1742-2132/9/6/655.
- [19] Pint JJ. (2003) *The Desert Caves of Saudi Arabia*: Stacey International, London, ISBN: 1 900988 48 8, 120 pp.
- [20] Wittaker BN. Reddish DJ. (1989) *Subsidence: Occurrence, Prediction and Control. Development in Geotechnical Engineering*, 56, Elsevier, 528 pp.
- [21] Davis SN. (1978) Origin of earth fissures. 74th Annual meeting, Tempe, Arizona, March 29–31, 1978. *Geological Society of America, Abstracts*, 10 (3), p 102.
- [22] Helm DC. (1994) Hydraulic forces that play a role in generating fissures at depth. *Bulletin Association Engineering Geologists*, 31:293–304.
- [23] Lofgren BE. (1978) Hydraulic stresses cause ground movement and fissures, Picacho, Arizona. *Geological Society American Abstracts Programs*, 10, p. 113.
- [24] Roobol MJ. Shouman SA. Al-Solami AM. (1985) Earth tremors, ground fractures, and damage to buildings at Tabah (22/42C): Saudi Arabian Deputy Ministry for Mineral Resources, Technical Record DGMR-TR-05-4, 46 pp.
- [25] Youssef AM. Maerz NH. (2013) Overview of some geological hazards in the Saudi Arabia. *Environment and Earth Science*, 70:3115–3130. Doi: 10.1007/s12665-013-2373-4.
- [26] Holzer TL. (1984) Ground failure induced by ground-water withdrawal from unconsolidated sediment. In Holzer TL (Ed). *Man-induced land subsidence*, Rev. Eng. Geol., VI, the Geological Soc. of America, 67–105.
- [27] Youssef AM. Sabtan AA. Maerz NH. Zabramawi YA. (2014) Earth Fissures in Wadi Najran, Kingdom of Saudi Arabia. *Natural Hazards*, 71:2013–2027. Doi: 10.1007/s11069-013-0991-5.
- [28] Lund W. Lowe M. Bowman S. (2010) *Land Subsidence and Earth Fissure Policy Recommendations*, Cedar Valley, Iron County, Utah, Utah Geological Survey.
- [29] Mousavi SM. Shamsai A. El Nagggar MH. Khomehchian M. (2001) A GPS-based monitoring program of land subsidence due to groundwater withdrawal in Iran. *Canadian Journal of Civil Engineering*, 28:452–464.
- [30] Sahu P. Sikdar PK. (2011) Threat of land subsidence in and around Kolkata City and East Kolkata Wetlands, West Bengal, India. *Journal of Earth System Science*, 120(3):435–446.
- [31] Sun H. Grandstaff D. Shagam R. (1999) Land subsidence due to groundwater withdrawal: potential damage of subsidence and sea level rise in southern New Jersey, USA. *Environmental Geology*, 37:290–296.

- [32] Wolkersdorfer Ch. Thiem G. (2006) Ground water withdrawal and land subsidence in Northeastern Saxony (Germany), Mine Water and Environment Association.
- [33] Xu YS. Shen SL. Cai ZY. Zhou GY. (2008) The state of land subsidence and prediction approaches due to groundwater withdrawal in China. *Natural Hazards*, 45(1):123–135.
- [34] Zhang Y. Xue YQ. Wu JC. Shi XQ. Yu J. (2010) Excessive groundwater withdrawal and resultant land subsidence in the Su-Xi-Chang area, China. *Environmental Earth Sciences*, 61(6):1135–1143.
- [35] Toufigh MM. Q`marsi K. (2002) Single well subsidence modeling based on finite element formulation, 2nd Canadian Specialty Conference on Computer Application in Geotechnique Proceeding, pp. 298–303.
- [36] Amin AA.(1988) Potential Geologic Hazards at the Village of Tabah, Hail Region, MSc thesis, KAAU, Jeddah, 164 pp.
- [37] Amin AA. Shehata WM.(1991) Subsidence due to groundwater withdrawal in a volcanic crater, Presented in Hazards 91, Session 11, Perugia, Italy.
- [38] Amin AA. Bankher K. (1995) Review on land subsidence in Saudi Arabia: in Barends, Brouwer and Schoder (Eds.), *Land Subsidence*, Balkema, Rotterdam, pp. 19–26.
- [39] Bankher K. (1996) Engineering Geological Evaluation of Earth Fissures in Wadi Al-Yutamah South Al-Madinah Al-Munawwarah, M.Sc. Unpublished thesis, FES, Jeddah.
- [40] Zabramawi YA. Youssef AM. Sabtan AA. Khiyami H. Bahamil AM. Al-Harbi HM. Hawsawi H. Zawahri M. Al-Wegdani K. (2009) Earth Fissures at Wadi Najran, Kingdom of Saudi Arabia: Saudi Geological Survey Technical Report SGS-TR-2009-12.
- [41] Bahamil AM. Youssef AM. Khiyami H. Bulkhi AB. Otaibi ZA. Alshaikhi EA. (2016) Investigate and Evaluate of the Earth Fissures at Hail, Al Jouf, and Al Qasim regions (Al Qasim Region), Kingdom of Saudi Arabia: Saudi Geological Survey Technical Report SGS-TR-2016-4.
- [42] Zabramawi YA. Youssef AM. Al-Harbi HM. Otaibi ZA. (2016) Investigate and evaluate of the Earth Fissures at Hail, Al Jouf, and Al Qasim regions (Hail Region), Kingdom of Saudi Arabia: Saudi Geological Survey Technical Report SGS-TR-2016-3.
- [43] Zahrani SA. Youssef AM. Bulkhi AB. Al-Harbi HM. Otaibi ZA. Aamri M. (2016) Investigate and Evaluate of the Earth Fissures at Hail, Al Jouf, and Al Qasim regions (Al Jouf Region), Kingdom of Saudi Arabia: Saudi Geological Survey Technical Report SGS-TR-2016-2.
- [44] Shehata W. Roobol JM. Stewart I. Khiyami H. Al Khammash A. Sayed S. Tarabolsi Y. Al Ahmadi K. (2007) Evaluation of a Subsidence Hazard in the Al Khafji area. Confidential report Saudi Geological Survey.
- [45] Peters WD. Pint JJ. Kremla N. (1990) Karst landforms in the Kingdom of Saudi Arabia. *The NSS Bulletin*, 52:21–32.

- [46] Vaslet D. Al-Muallem MS. Maddah SS. Brosse JM. Fourniguet J. Breton JP. Le Nindre YM. (1991) Geologic Map of the Ar Riyadh Quadrangle, Sheet 24 I, Scale 1:250,000, Kingdom of Saudi Arabia: Saudi Arabian Deputy Ministry for Mineral Resources Geoscience Map GM-121, 54 pp.
- [47] Dini SM. Wallace CA. Halawani MA. Al-Sobhi SA. Kashghari WA. Al-Ghamdi AS. (2009) Geologic map of the as Sulayyil Quadrangle, Sheet 20H, Scale 1:250,000. Kingdom of Saudi Arabia. Saudi Geological Survey 64 pp.
- [48] Memesh AM. Dini SM. Gutiérrez F. Wallace CA. (2008) Evidence of Large-Scale Subsidence Caused by Interstratal Karstification of Evaporites in the Interior Homocline of Central Saudi Arabia. European Geosciences Union General Assembly Geophysical Research Abstracts 10: A-02276.
- [49] Dini SM. Al-Khattabi AF. Wallace CA. Banakhar AS. Al-Kaff MH. Al-Garni SM (2007) Geologic Map of Parts of the Judayyidet 'Ar'Ar Quadrangle, Sheet 31E, and Faydat al Adyan Quadrangle, Sheet 31F, Scale 1:250,000. Kingdom of Saudi Arabia. Saudi Geological Survey 45 pp.
- [50] Al-Khattabi AF. Dini SM. Wallace CA. Banakhar AS. Al-Kaff MH. Al-Zahrani AM. (2010) Geologic Map of Parts of the 'Ar'Ar Quadrangle, Sheet 30E, Scale 1:250,000. Kingdom of Saudi Arabia. Saudi Geological Survey 50 pp.
- [51] Gutiérrez F. Cooper AH. Johnson KS. (2008a) Identification, prediction and mitigation of sinkhole hazards in evaporite karst areas. *Environmental Geology*, 53:1007–1022.
- [52] Gutiérrez F. Guerrero J. Lucha P. (2008b) A genetic classification of sinkholes illustrated from evaporite paleokarst exposures in Spain. *Environmental Geology*, 53:993–1006.
- [53] Gutiérrez F. Parise M. De Waele J. Jourde H. (2014b) A review on natural and human-induced geohazards and impacts in karst. *Earth Science Reviews*, 138:61–88.
- [54] Wallace CA. Dini SM. Al-Farasani AA. (2000b) Geological Map of the Wadi Sirhan Quadrangle, Sheet 30C, Kingdom of Saudi Arabia: Saudi Geological Survey Geoscience Map GM-127C, scale 1: 250,000.
- [55] Banakhar AS. Al Zahrani AM. Al-Juaid AJ. Dini SM. Wallace CA. Al-Kaff MH. Al-Tassan AA. (2011) Geologic Map of the Markaz Adhfa Quadrangle, Sheet 29E, Scale 1:250,000. Kingdom of Saudi Arabia. Saudi Geological Survey, Geoscience Map GM-144C.
- [56] Manivit J. Vaslet D. Berthiaux A. Le Strat P. Fourniguet J. (1986) Geological Map of the Buraydah Quadrangle, Sheet 26G. Kingdom of Saudi Arabia (with text): Saudi Arabia Deputy Ministry for Mineral Resources Geoscience Map GM-114C, scale 1: 250,000.

- [57] Pint JJ. (2009) The Lava Caves of Khaybar, Saudi Arabia. Proceedings of the 15th International Congress of Speleology, Kerrville, Texas, 1873–1878.
- [58] Powers RW. Ramirez LF. Redmond CD. Elberg JrFL. (1966) Geology of the Arabian Peninsula: Sedimentary Geology of Saudi Arabia. U.S. Geological Survey Professional Paper 560-D.
- [59] Memesh AM. Dini SM. Al-Amoudi SA. Wallace CA. Sobhi SA. Al-Juaid AJ. (2010) Geologic Map of the Hawtat Bani Tamim Quadrangle, Sheet 21I, Sscale 1:250,000. Kingdom of Saudi Arabia. Saudi Geological Survey 64 pp.
- [60] Zabramawi YA. Youssef AM. Qalioubi H. Memish A. (2011) Investigate and evaluate the karst problems along Al Atailiyah road, Kingdom of Saudi Arabia: Saudi Geological Survey, Technical Report SGS-TR-2011-1.
- [61] Zabramawi YA. Youssef AM. Bahamil AM. Al Amri RM. Otaibi ZA. (2015) Investigate and Evaluate of the Karst Problems at Essawiyah Area. Kingdom of Saudi Arabia: Saudi Geological Survey, Technical Report SGS-TR-2015-11.
- [62] Bulkhi AB. Youssef AM. Sabtan AA. Al-Harathi SG. Baamer MF. Al-Wegdani K. Al-Shereif A.(2009) Study and Surveying to Determine the Causes of Karstification in Al Aizizyah Area, Reyad, Kingdom of Saudi Arabia: Saudi Geological Survey Technical Report SGS-CR-2009-3.
- [63] Carbonel D. Rodríguez-Tribaldos V. Gutiérrez F. Galve JP. Guerrero J. Zaroca M. Roqué C. Linares R. McCalpin JP. Acosta E. (2015) Investigating a damaging buried sinkhole cluster in an urban area integrating multiple techniques: geomorphological surveys, DInSAR, GPR, ERT, and trenching. *Geomorphology*, 229:3–16.
- [64] Gutiérrez F. Galve JP. Lucha P. Castañeda C. Bonachea J. Guerrero J. (2011) Integrating geomorphological mapping, trenching, InSAR and GPR for the identification and characterization of sinkholes in the mantled evaporite karst of the Ebro Valley (NE Spain). *Geomorphology*, 134:144–156.
- [65] McCalpin J. (2009) *Paleoseismology*, Second Edition. Academic Press. 629 pp. eBook ISBN: 9780080919980.
- [66] Gutiérrez F. Galve JP. Lucha P. Bonachea J. Jordá L. Jordá R. (2009) Investigation of a large collapse sinkhole affecting a multi-storey building by means of geophysics and the trenching technique (Zaragoza city, NE Spain). *Environmental Geology*, 58:1107–1122.
- [67] Gutiérrez F. Lucha P. Galve JP. (2010) Reconstructing the geochronological evolution of large landslides by means of the trenching technique in the Yesa Reservoir (Spanish Pyrenees). *Geomorphology*, 124:124–136.
- [68] Carbonel D. Rosdríguez V. Gutiérrez F. McCalpin JP. Linares R. Roqué C. Zarroca M. Guerrero J. (2014) Sinkhole characterisation combining trenching, Ground Penetrating

Radar (GPR) and Electrical Resistivity Tomography (ERT). *Earth Surface Processes and Landforms*, 39:214–227.

- [69] Griffiths DH. Barker RD. (1993) Two-dimensional resistivity imaging and modeling in areas of complex geology. *Journal of Applied Geophysics*, 29:211–226. Doi: 10.1016/0926-9851(93)90005-J.
- [70] Gambetta M. Armadillo E. Carmisciano C. Stefanelli P. Cocchi L. Tontini FC. (2011) Determining geophysical properties of a near surface cave through integrated micro-gravity vertical gradient and electrical resistivity tomography measurements. *Journal of Cave and Karst Studies*, 73(1):11–15. Doi: 10.4311/jcks2009ex0091.
- [71] Lambert DW. (1997) Dipole-Dipole D.C. Resistivity Surveying for Exploration of Karst Features. *The Engineering Geology and Hydrogeology of Karst Terranes, Proceedings of the Sixth Multidisciplinary Conference on Sinkholes and the Engineering and Environmental Impacts of Karst, Springfield, Missouri, April 6–9*. pp. 413–418.
- [72] Roth MJS. Nyquist JE. (2003) Evaluation of Multi-Electrode Earth Resistivity Testing in Karst. *Geotechnical Testing Journal, ASTM*, 26:167–178.
- [73] Van Schoor M. (2002) Detection of sinkholes using 2D electrical resistivity imaging. *Journal of Applied Geophysics*, 50:393–399.
- [74] Zhou W. Beck BF. Adams AL. (2002) Effective electrode array in mapping karst hazards in electrical resistivity tomography. *Environmental Geology*, 42:922–928. Doi: 10.1007/s00254-002-0594-z.
- [75] Zabramawi YA. Khiyami H. Youssef AM. Sabtan AA. Al-Harhi SG. Memash A. Al-Sharef A. Al-Ahmadi KZ. (2009) Karst Investigation and Analysis in An Nu'ayriyah Area, Kingdom of Saudi Arabia. Saudi Geological Survey Technical Report SGS-TR-2009-6.

IntechOpen

